Quantum Nano-Electronics

Hervé Courtois

Institut Néel
CNRS, Université Joseph Fourier and Grenoble INP

http://neel.cnrs.fr/spip.php?article804&lang=en
herve.courtois@neel.cnrs.fr

Outline:

Tunneling phenomena: from the planar junctions to the STM

Quantum nano-electronic devices: single-electron effects, Josephson junctions, quantum bits

Quantum transport: Landauer formalism, Aharonov-Bohm effect, weak localization, noise

Mesoscopic superconductivity

Part 1
Tunneling phenomena: from the planar junctions to the STM

Objective: to understand the electron tunnelling effect (including theory), learn the history of STM.

Chapter 1
Tunneling phenomena : from the planar junctions to the STM

1.1: The electronic density of states

The free electrons model

Uniform potential for electrons in a metal : free electrons in a box.

Consider their kinetic energy:

$$p = mv = \hbar k \qquad E_c = \frac{(\hbar k)^2}{2m} \qquad (k = \text{wave-vector})$$

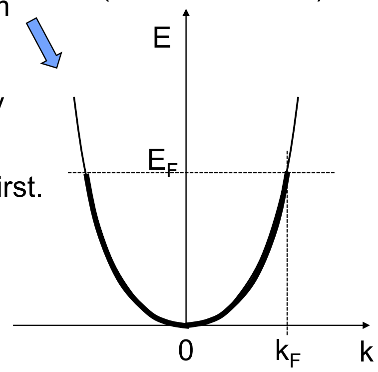

Pauli exclusion principle for Fermions: only two electrons per state (opposite spins).

Electrons occupy states of lowest energy first.

Fermi level = last occupied state at T = 0.

Fermi level energy E_F = electron chemical potential.

Counting electron states (1)

An energy below E_F means a wave-vector magnitude below k_F.

Number of states in the k-space inside the Fermi sphere of radius k_F ?

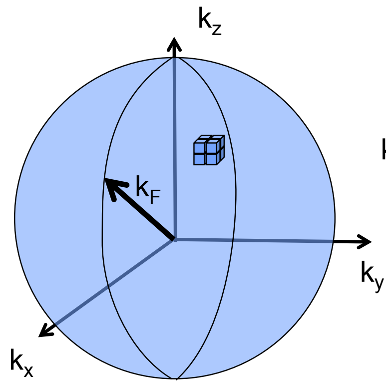

Boundary conditions for electrons in a box of dimensions L_x, L_y, L_z:

$$k_x = \frac{2\pi m_x}{L_x};\ k_y = \frac{2\pi m_y}{L_y};\ k_z = \frac{2\pi m_z}{L_z}$$

m_x, m_y, m_z are integers

One state occupies a parallepiped of volume $(2\pi)^3/L_xL_yL_z$, two electrons per state.

Counting electron states (2)

Number of possible values for (m_x, m_y, m_z) within the Fermi sphere:

$$\underset{\text{spin}}{2}\,\frac{4\pi k_F^3/3}{(2\pi)^3/L_xL_yL_z} = \frac{V}{3\pi^2}k_F^3 = n_F \quad \Rightarrow \quad k_F = \left(\frac{3\pi^2 n_F}{V}\right)^{1/3}$$

n = number of electrons in a metal of volume V, Fermi wave-vector k_F.

The Fermi energy is then: $E_F = \dfrac{(\hbar k_F)^2}{2m} = \dfrac{\hbar^2}{2m}\left(\dfrac{3\pi^2 n_F}{V}\right)^{2/3}$

Number of electrons with an energy below E in a volume V:

$$n(E) = \frac{V}{3\pi^2}\left(\frac{2mE}{\hbar^2}\right)^{3/2}$$

The electronic density of states

The electronic Density Of States (DOS) gives the number of states per unit volume and unit energy at a given energy E:

$$\boxed{N(E) = \frac{1}{V}\frac{dn(E)}{dE}}$$

In energy window of width dE, we have dN states per unit volume:

$$\boxed{dN = N(E)\,dE}$$

In a free electrons model, we have: $N(E) = \dfrac{m}{\hbar^2\pi^2}\sqrt{\dfrac{2mE}{\hbar^2}}$

DOS in “real“ materials usually differ from above expression.

DOS is usually spatially averaged.

With a local probe, one gets the Local Density Of States: LDOS.

"Good" metals

In a free electrons model, we have: $N(E) = \frac{m}{\hbar^2 \pi^2} \sqrt{\frac{2mE}{\hbar^2}}$

Varies slowly with energy $\frac{dN}{N} = \frac{dE}{2E_F}$

dE is eV, $k_B T$

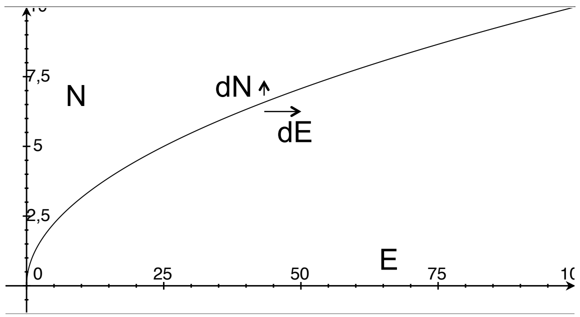

Chapter 1
Tunneling phenomena : from the planar junctions to the STM

1.2: The electronic work-function

The work-function of a metal (1)

Vacuum states are states with the electron out of the metal.

Definition: the work-function W is the energy needed for an electron to leave the metal.

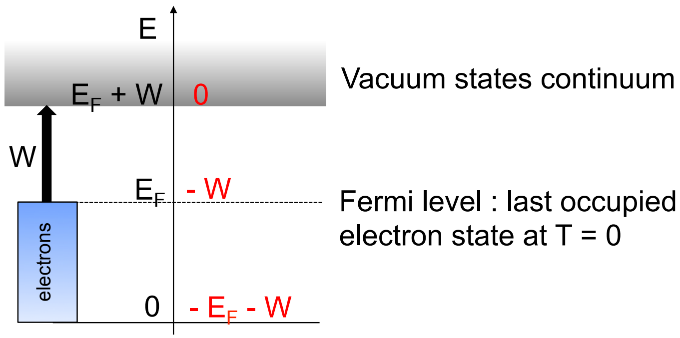

Reference energy taken at zero kinetic energy in the metal (black scale), can be chosen also in the vacuum (red), W inchanged.

The work-function of a metal (2)

The photo-electric effect:
the photon hypothesis of Planck confirmed by Einstein

Frequency threshold for the photoelectric effect:

$h\nu = W$

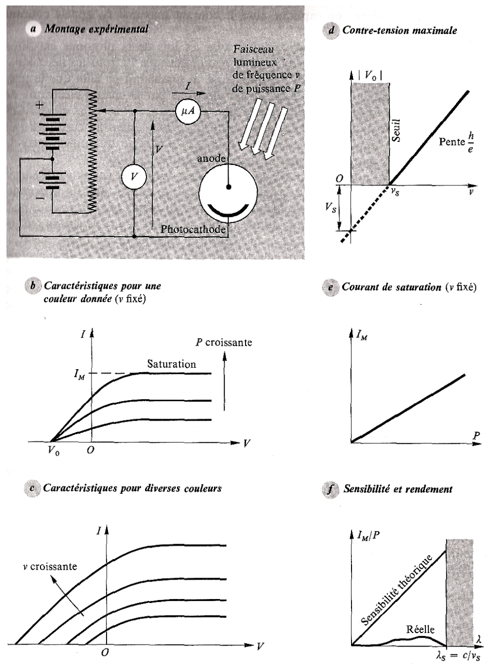

Measurement of the work-function

- Photo-electric effect

- Thermo-ionic emission (e- beam source in SEM, evaporators)

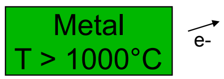

$$j \propto T^2 \exp\left(-\frac{W}{k_B T}\right)$$

- Kelvin probe

Values :

Metal	W (eV)
Li	2.38
Cu	4.4
Au	4.3
Hg	4.52
Al	4.25
W	4.5

Chapter 1
Tunneling phenomena: from the planar junctions to the STM

1.3: The basic “square barrier model“

The square barrier model

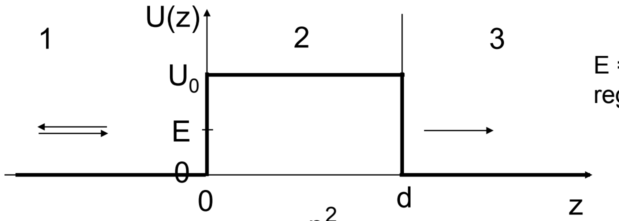

E = kinetic energy in region 1, where U = 0

Classical mechanics : $\frac{p_z^2}{2m} + U(z) = E$

One needs E > U(z) for the e^- to sit at a given point.
If E < W, the e^- stays in region 1.

Quantum mechanics : wave-function description satisfying the Shrödinger equation

$$\frac{-\hbar^2}{2m}\frac{d^2\psi}{dz^2} + U(z)\psi(z) = E\psi(z)$$

The particle current

Particle density is: $\rho = |\psi|^2$

The particle current defined as: $\vec{j} = \frac{-i\hbar}{2m}\left[\psi^* \vec{\nabla}\psi - \psi\vec{\nabla}\psi^*\right]$

obeys the conservation law: $\frac{\partial \rho}{\partial t} + \mathrm{div}\ \vec{j} = 0$

Simple case, the plane wave: $\psi(x) = A\, e^{ikx}$

The particle current is then: $\vec{j} = \frac{\hbar \vec{k}}{m}|A|^2 = \vec{v}|A|^2$

Demonstration through Shrödinger eq.: Cohen-Tanoudji p 239

The square barrier transmission

In 1 (z < 0): $\psi_1(z) = e^{ikz} + A\,.\,e^{-ikz}$ where $k = \dfrac{\sqrt{2mE}}{\hbar}$

In 2 (0 < z < d): $\psi_2(z) = B\,.\,e^{\alpha z} + C\,.\,e^{-\alpha z}$ where $\alpha = \dfrac{\sqrt{2m(U_0 - E)}}{\hbar}$

In 3 (d < z): $\psi_3(z) = De^{ikz}$

Continuity of ψ and its spatial derivative $d\psi/dz$:
4 equations provide the determination of A, B, C and D.

The transmission coefficient is:

$$T = \left|\frac{D}{1}\right|^2 = \frac{1}{1 + \dfrac{U_0^2}{4E(U_0 - E)}\,\mathrm{sh}^2(\alpha d)}$$

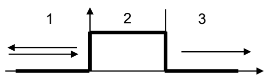

The thick barrier approximation

$$T = \left|\frac{D}{1}\right|^2 = \frac{1}{1 + \dfrac{U_0^2}{4E(U_0 - E)}\,\mathrm{sh}^2(\alpha d)}$$

Thick barrier approximation ($\alpha d >> 1$):

$$T \approx 16\frac{E(U_0 - E)}{U_0{}^2} e^{-2\alpha d}$$

Exponential decay of the transmission amplitude:

$$\boxed{T \propto \exp(-2\alpha d)}$$

A first order of magnitude

Order of magnitude: a man of mass m = 100 kg, a wall h = 4 m high, thickness = d

Energy barrier = mgh

$$T = \exp\left(-\frac{\sqrt{2.100.100.9{,}81.4}}{1{,}05.10^{-34}}d\right) = \exp\left(-10^{37}d\right)$$

T vanishing even with d down to Å scale.

The case of electrons

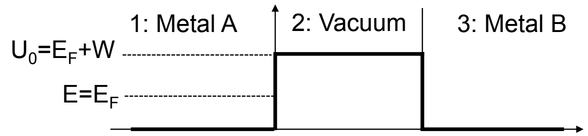

$E \approx E_F$

$U_0 = E_F + W$ ⇒ $\alpha = \dfrac{\sqrt{2mW}}{\hbar}$ $\quad T \approx 16\dfrac{E_F W}{(E_F + W)^2} e^{-2\alpha d} \propto \exp(-2\alpha d)$

Order of magnitude: $T = \exp\left(-\dfrac{\sqrt{2.9{,}1.10^{-31}.4.1{,}6.10^{-19}}}{1{,}05.10^{-34}}d\right) = \exp\left(-10^{10}d\right)$

Thanks to the low electron mass and low energy barrier:
T is non negligible for d of the order of the Å.

Tunneling vs conduction

How large can a tunnel current be ?

Mesoscopic transport: $I = G_Q V \sum_{\text{channel } i} T_i$

Quantum conductance: $G_Q = \frac{2e^2}{h} = \frac{1}{12.9\ \text{k}\Omega}$ (includes spin)

Diffusive transport: T is close to 1.

Tunnel effect: T is “small“.

With V = 0.13 V, T = 10^{-4} for one channel: I = 1 nA

Transmission through an arbitrary barrier

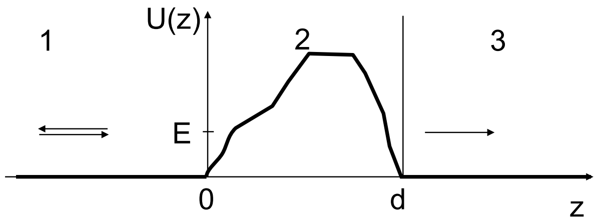

WKB (Wentzel, Kramers and Brillouin) semiclassical approximation (slow spatial variation of the wave-function amplitude, no local minima):

$$\boxed{T \propto \exp\left(-\frac{2}{\hbar}\int_0^d \left\{\left[2m\left(U(z)-E\right)\right]^{1/2} dz\right\}\right)}$$

Coincides with barrier model result in this special case.

Arbitrary barrier: WKB result interpretation

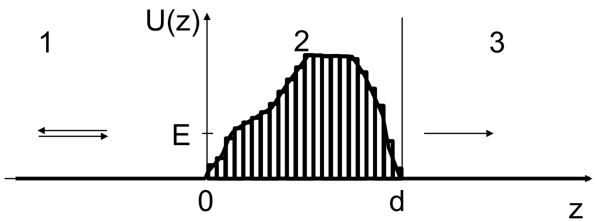

Decomposition of the barrier into square (rectangular) barriers, local height $U(z_i)$, width dz:

$$T_i \propto \exp\left(-\frac{2}{\hbar}\left[2m\left(U(z_i)-E\right)\right]^{1/2} dz\right)$$

Total transmission: $T = \prod T_i \propto \prod \exp\left(-\frac{2}{\hbar}\left[2m\left(U(z_i)-E\right)\right]^{1/2} dz\right)$

$$T \propto \exp\left(-\frac{2}{\hbar}\sum\left[2m\left(U(z_i)-E\right)\right]^{1/2} dz\right) \approx \exp\left(-\frac{2}{\hbar}\int_0^d \left\{\left[2m\left(U(z)-E\right)\right]^{1/2} dz\right\}\right)$$

Chapter 1
Tunneling phenomena: from the planar junctions to the STM

1.4: A microscopic picture

Microscopic view

Tunnel matrix element describes the overlap of the electronic wave-functions:

$$\boxed{M_{\psi\chi} = \iint_S \left(\chi^* \frac{\partial \psi}{\partial z} - \psi \frac{\partial \chi^*}{\partial z} \right) dS}$$

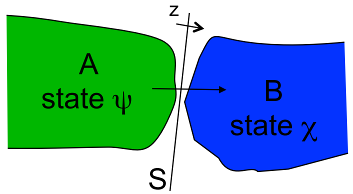

Hypothesis: Electron states χ and ψ are not affected by the tunnel contact.
Bardeen, 1964

Integral over any surface S in the vacuum between the two metals, depends obviously on distance between A and B.
z = normal to the surface S.

Tunneling probability

The Fermi golden rule gives the transition probability from a state ψ to a state χ:

$$\boxed{p_{\psi\to\chi} = \frac{2\pi}{\hbar}\left|\langle\psi|H_T|\chi\rangle\right|^2 \delta\left(E_\psi - E_\chi\right) = \frac{2\pi}{\hbar}\left|M_{\psi\chi}\right|^2 \delta\left(E_\psi - E_\chi\right)}$$

Valid for every couple of states (state in metal A, state in metal B).

The $|M_{\psi\chi}|^2$ term includes the distance dependence.

The tunneling effect is elastic to first order (no energy exchange).

Inelastic tunneling rate is only about 10^{-5} of the elastic rate.

$\delta(x)$ = Dirac delta function (= 0 except if x = 0). $\int_{-\infty}^{+\infty} f(x)\delta(x) = f(0)$

Chapter 1
Tunneling phenomena: from the planar junctions to the STM

1.5: The tunneling current

Equilibrium situation

Consider two metals with a voltage bias in-between.

At zero bias, the two FL get aligned.

Plot the DOS, occupied states at T = 0 are colored.

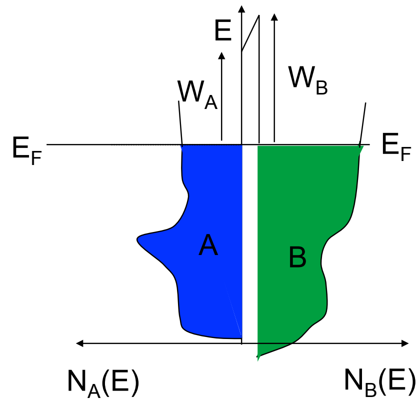

N_A, N_B: Local Density Of (electronic) States (LDOS) of metal A or B.

If different work-functions $W_A \neq W_B$:

non-zero electric field between the metals, cf KFM.

With a voltage bias

Consider two metals with a voltage bias in-between.
At zero bias, the two FL get aligned.
Plot the DOS, occupied states at T = 0 are colored.

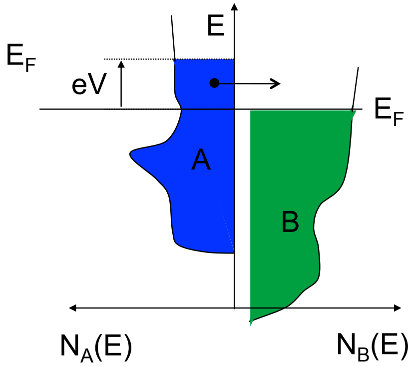

N_A, N_B: Local Density Of (electronic) States (LDOS) of metal A or B.

Voltage bias V: shifts the FLs.
$N_A(E) \Rightarrow N_A(E\text{-}eV)$

Elastic electron tunneling:
"Horizontal" process.

Electron energy relaxation

After the electron is transmitted, it **will** relax to lower energy
Thanks to inelastic processes with e-, phonons, …
Separate process from tunneling, much longer times involved.

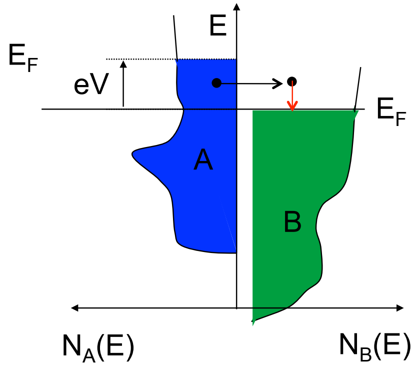

The energy distribution function

Non-zero temperature: the energy distribution function f(E) gives the probability for an e^- state at the energy E to be occupied.

At thermal equilibrium, f is the Fermi-Dirac function:

$$f(E) = \frac{1}{1 + \exp\left[\frac{E - E_F}{k_B T}\right]}$$

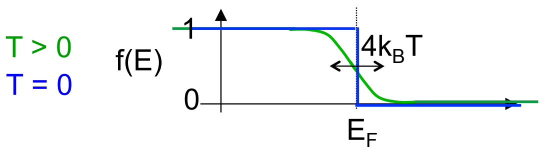

At zero temperature, it reduces to a step function.

At non-zero temperature

Non-zero temperature, the number of electrons within a window dE at an energy E is:

$$\boxed{dN = N(E)\, f(E) dE}$$

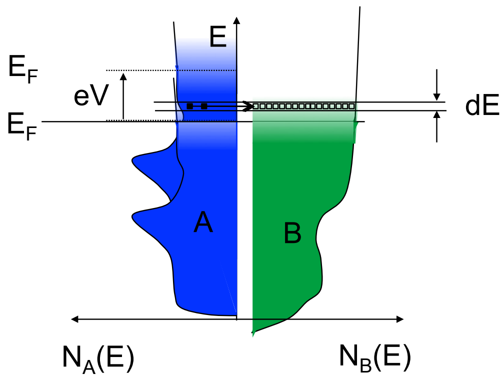

Consider an energy window [E;E+dE] and determine the electron flow from A to B.

The tunnel current expression (2)

What's the electron flow from A to B ?

Number of occupied states in A at the energy E = $N_A(E-eV)f(E-eV)dE$

Number of free states in B at the energy E'= $N_B(E')[1-f(E')]dE'$

Tunnel current element (Fermi golden rule):

$$d^2I_{A\to B} = \underbrace{2}_{\text{spin}}e\underbrace{\frac{2\pi}{\hbar}|M_{AB}|^2}_{p}\delta(E-E')N_A(E-eV)N_B(E')f(E-eV)[1-f(E')]dEdE'$$

$$dI_{A\to B} = 2e\frac{2\pi}{\hbar}|M_{AB}|^2\int_{E'=-\infty}^{+\infty}\delta(E-E')N_A(E-eV)N_B(E')f(E-eV)[1-f(E')]dEdE'$$

$$dI_{A\to B} = 2e\frac{2\pi}{\hbar}|M_{AB}|^2 N_A(E-eV)N_B(E)f(E-eV)[1-f(E)]dE$$

The tunnel current expression (3)

Net current, with the hypothesis that M depends only on E:

$$dI = dI_{A\to B} - dI_{B\to A}$$

$$= \frac{4\pi e}{\hbar}|M(E)|^2 N_A(E-eV)N_B(E)\{f(E-eV)[1-f(E)]-f(E)[1-f(E-eV)]\}dE$$

$$= \frac{4\pi e}{\hbar}|M(E)|^2 N_A(E-eV)N_B(E)[f(E-eV)-f(E)]dE$$

Total current :

$$\boxed{I = \int_{-\infty}^{+\infty} dI = \frac{4\pi e}{\hbar}\int_{-\infty}^{+\infty}|M(E)|^2 N_A(E-eV)N_B(E)[f(E-eV)-f(E)]dE}$$

Interpretation: a tunnel current occurs because of an electron states occupancy (at a given energy) difference.

The tunneling spectroscopy (1)

$$\boxed{I = \int_{-\infty}^{+\infty} dI = \frac{4\pi e}{\hbar}\int_{-\infty}^{+\infty}|M(E)|^2 N_A(E-eV)N_B(E)[f(E-eV)-f(E)]dE}$$

If A (the tip) is a good metal : $N_A(E)$ = Constant.

Hypothesis: M(E) = Constant (eV << W).

$$\boxed{I \propto \int_{-\infty}^{+\infty} N_B(E)[f(E-eV)-f(E)]dE}$$

The tunneling spectroscopy (2)

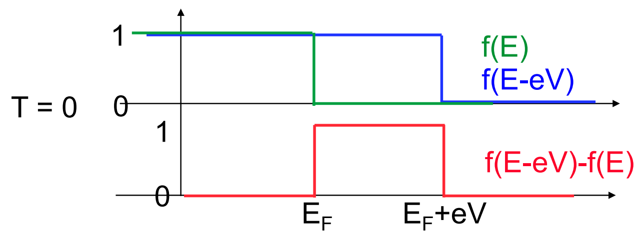

At T = 0

$$I \propto \int_{E_F}^{E_F+eV} N_B(E)dE$$

Calculating the derivative with respect to voltage provides the differential conductance, which is a function of voltage bias.

$$\boxed{\frac{dI}{dV}(V) \propto N_B(E_F+eV)}$$

energy scale defined by voltage bias

The zero-temperature differential conductance measures the LDOS.

Assumptions: tip DOS, constant M(E) for states involved.

If N_B = Cste, dI/dV = Cste, Ohm's law recovered (valid also at T > 0).

The tunneling spectroscopy (3)

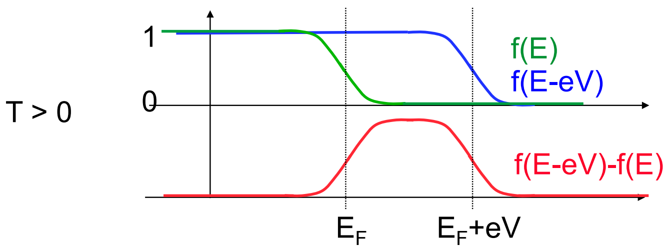

$$\frac{dI}{dV} \propto \int_{-\infty}^{+\infty} N_B(E)\frac{d}{dV}\big(f(E-eV)\big)dE \propto \int_{-\infty}^{+\infty} \frac{e}{4k_BT}\cosh^{-2}\left(\frac{E-E_F-eV}{k_BT}\right)N_B(E)dE$$

thermal equilibrium is assumed: f is the Fermi-Dirac function

The tunneling spectroscopy (4)

$$\frac{dI}{dV} \propto \int_{-\infty}^{+\infty} \frac{e}{4k_BT}\cosh^{-2}\left(\frac{E-E_F-eV}{k_BT}\right)N_B(E)dE$$

Plot of $\frac{1}{T}\cosh^{-2}\left(\frac{E-eV}{k_BT}\right)$ for different temperatures

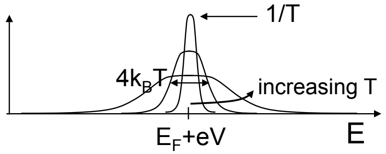

T = 0: window function is $\delta(E - eV)$, one recovers dI/dV(V) = $N_B(E_F+eV)$.

T > 0: thermal window of half-width $2k_BT$.

The diff. cond. dI/dV gives the LDOS $N_B(E)$ smeared by temperature.

Tunneling spectroscopy resolution = 2 k_BT: 1 K gives 0.17 meV.

Chapter 1
Tunneling phenomena: from the planar junctions to the STM

1.6: History of electron tunneling

Elements of superconductivity (1)

A superconductor below T_c: zero resistance, perfect diamagnetism (B=0)

Condensation of electrons into Cooper pairs: modified DOS at the FL

BCS (from Bardeen-Cooper-Schrieffer) theory, the DOS writes:

$$N_S(E) = 0 \quad \text{if } |E - E_F| < \Delta$$

$$N_S(E) = N_N \frac{|E|}{\sqrt{(E-E_F)^2 - \Delta^2}} \quad \text{if } |E - E_F| > \Delta$$

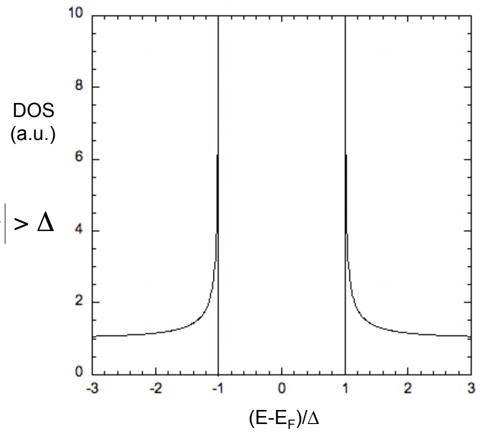

The energy gap is :
$\Delta(T=0) = 1.76k_BT_c$

Thermal smearing of a LDOS

Example:
BCS DOS +
smearing

High resolution means
small smearing, implies
low temperature.

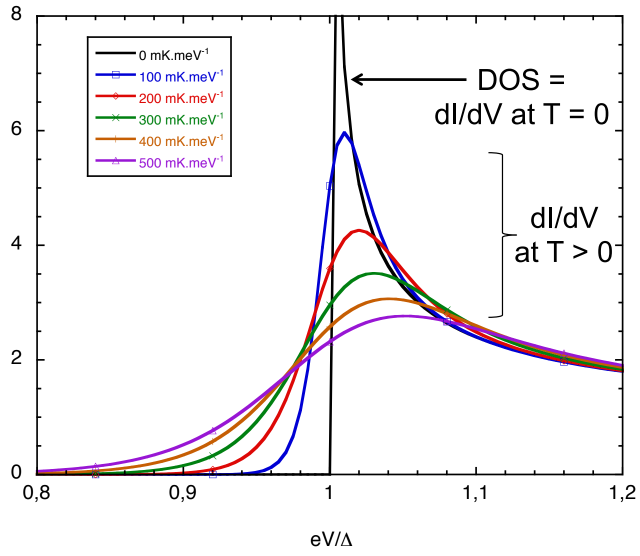

Tunneling before the STM (1)

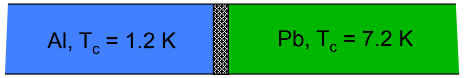

Al_2O_3 insulating barrier (a few nm):
equivalent to vacuum tunneling.

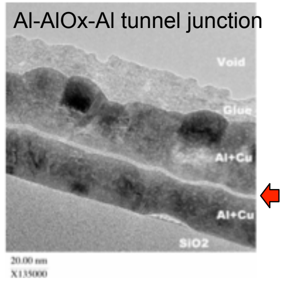

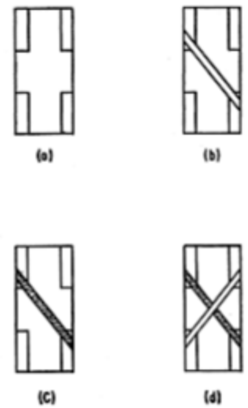

FIG. 3. Sample preparation. (a) Glass slide with indium contacts. (b) An aluminum strip has been deposited across the contacts. (c) The aluminum strip has been oxidized. (d) A lead film has been deposited across the aluminum film, forming an $Al\text{-}Al_2O_3\text{-}Pb$ sandwich.

Tunneling in planar, solid-state junctions:
straightforward stability.

I. Giaever, Phys. Rev. Lett. 5, 147 (1960)
Nobel prize 1973

Tunneling before the STM (2)

I. Giaever, Phys. Rev. Lett. 5, 147 (1960).

Temperature regime where Pb is superconducting, Al normal.

First direct measurement of a superconducting DOS.

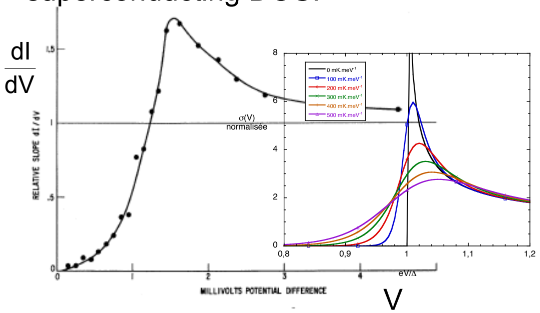

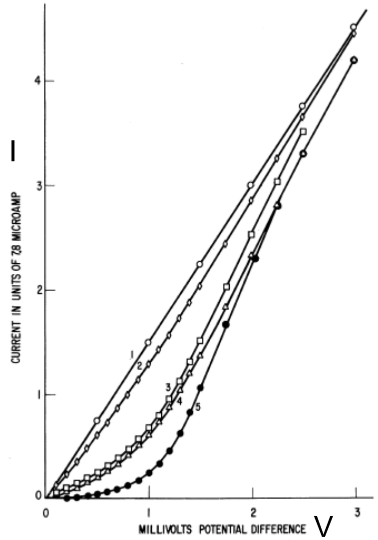

FIG. 1. Tunnel current between Al and Pb through Al_2O_3 film as a function of voltage. (1) $T=4.2°K$ and $1.6°K$, $H=2.7$ koe (Pb normal). (2) $T=4.2°K$, $H=0.8$ koe. (3) $T=1.6°K$, $H=0.8$ koe. (4) $T=4.2°K$, $H=0$ (Pb superconducting). (5) $T=1.6°K$, $H=0$ (Pb superconducting).

Chapter 1
Tunneling phenomena: from the planar junctions to the STM

1.7: The field emission regime

Field emission (1)

A sharp tip biased with a negative voltage :
What is the electric field at the tip apex ?

$$\boxed{E_{el} \approx \frac{V}{r}}$$

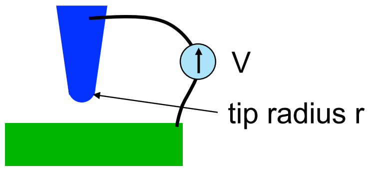

1 Volt and 10 nm give 10^{10} V/m = 1 V/Å
>> ionization field in air (3.10^6 V/m)

Huge electric fields :
unusual physics at the tip apex like atom migration.

Field emission (2)

Metallic tip at a negative potential:

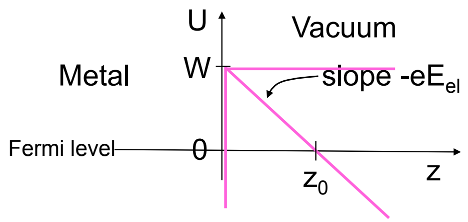

$$U(z) = W - eE_{el}z$$

$$U(z_0) = 0 \Rightarrow z_0 = \frac{W}{eE_{el}}$$

Tunneling through an electric field-induced barrier: no sample needed !

Result from WKB semiclassical approximation:

$$\boxed{T_{FE} \propto \exp\left(-\frac{4\sqrt{2m}}{3e\hbar}\frac{W^{3/2}}{E_{el}}\right)}$$

Used in electron beam sources (SEMs): smaller beam size, long tip life.

Transmission probabilities in practical units

W in eV
E_{el} in V/Å
d in Å
These quantities are of order 1 to 10.

Vacuum tunneling between two metals: $T_{VT} \propto \exp\left(-1.02W^{1/2}d\right)$

Field emission: $T_{FE} \propto \exp\left(-0.68\frac{W^{3/2}}{E_{el}}\right)$

Transmission coefficients are then of order 10^{-1} to 10^{-10}.

No distance dependence for T_{FE}: transmission depends on bias.
No field dependence for T_{VT}: Ohmic behavior expected.

Field emission versus vacuum tunneling

Between a tip and a sample at different distances:

At large distance, field emission dominates. Appears only at high voltage when el. field is large: non-linear behaviour. Also called Fowler-Nordheim regime.

At short distance, usual tunnel current dominates, ohmic behaviour.

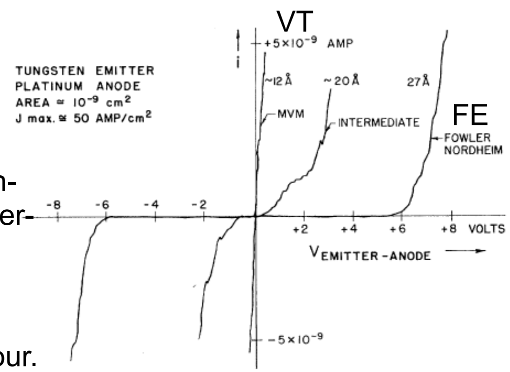

FIG. 3. Tunneling current versus voltage characteristic for three different emitter-to-surface spacings. Note the linear MVM characteristic.

R. Young et al., Phys. Rev. Lett. 27, 922 (1971)

The first scanning probe microscope ever

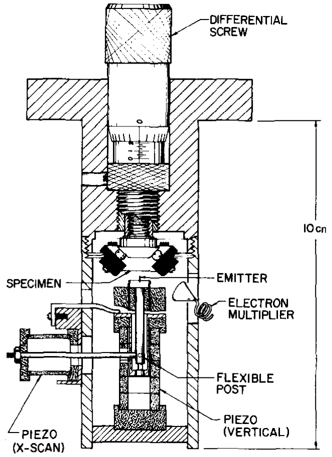

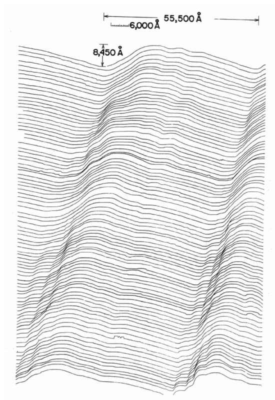

Image of a Au grating: resolution not better than an optical image.

The “topografiner“: the first scanning probe microscope.

R. Young et al., Phys. Rev. Lett. 27, 922 (1971)

Chapter 1
Tunneling phenomena: from the planar junctions to the STM

1.8: The invention of STM

The invention of STM (1)

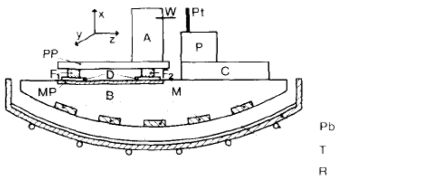

FIG. 1. Schematic of the tunneling unit and magnetic levitation system. Components and operation are described in the text. Liquid-He circulating in the tubes T cools the lead bowl Pb, which is thermally shielded by Al-coated mylar foils (not shown).

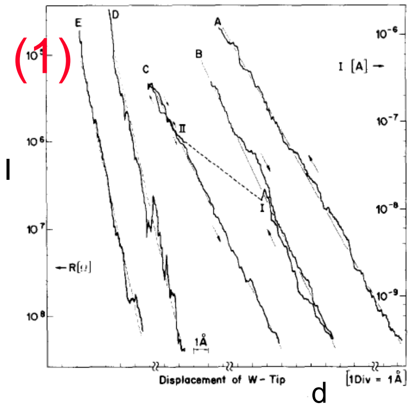

FIG. 2. Tunnel resistance and current vs displacement of Pt plate for different surface conditions as described in the text. The displacement origin is arbitrary for each curve (except for curves B and C with the same origin). The sweep rate was approximately 1 Å/s. Work functions $\phi = 0.6$ eV and 0.7 eV are derived from curves A, B, and C, respectively. The instability which occurred while scanning B and resulted in a jump from point I to II is attributed to the release of thermal stress in the unit. After this, the tunnel unit remained stable within 0.2 Å as shown by curve C. After repeated cleaning and in slightly better vacuum, the steepness of curves D and E resulted in $\phi = 3.2$ eV.

Demonstration of vacuum tunneling.

The apparent work-function depends on the tip condition (contamination).

“Tunneling through a controllable vacuum gap”, G. Binnig, H. Röhrer, Ch. Gerber and E. Weibel, Appl. Phys. Lett. 40, 178 (1982).

The invention of STM (2)

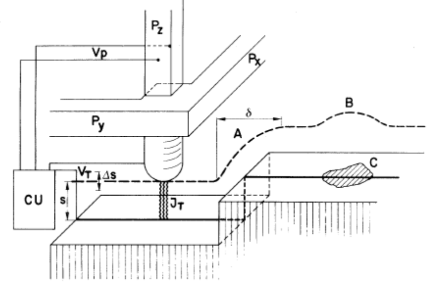

FIG. 1. Principle of operation of the scanning tunneling microscope. (Schematic: distances and sizes are not to scale.) The piezodrives P_x and P_y scan the metal tip M over the surface. The control unit (CU) applies the appropriate voltage V_p to the piezodrive P_z for constant tunnel current J_T at constant tunnel voltage V_T. For constant work function, the voltages applied to the piezodrives P_x, P_y, and P_z yield the topography of the surface directly, whereas modulation of the tunnel distance s by Δs gives a measure of the work function as explained in the text. The broken line indicates the z displacement in a y scan at (A) a surface step and (B) a contamination spot, C, with lower work function.

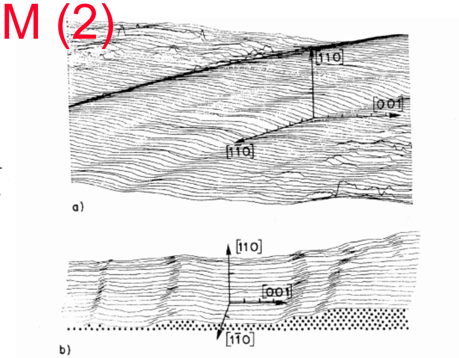

FIG. 3. Two examples of scanning tunneling micrographs of a Au (110) surface, taken at (a) room temperature, and (b) 300°C after annealing for 20 h at the same temperature (and essentially constant work function). The sensitivity is 10 Å/div everywhere. Because of a small thermal drift, there is some uncertainty in the crystal directions in the surface. In (a), the surface is gently corrugated in the [001] direction, except for a step of four atomic layers (≅ 2 atomic radii) along the [1̄10] direction, as indicated by the discontinuity of the shaded ribbon. The steps in (b), which were always found along the [11̄0] direction, are visualized by the possible positions of the Au atoms (dots).

“Surface studies by scanning tunneling microscopy”, G. Binnig, H. Röhrer, Ch. Gerber and E. Weibel, Phys. Rev. Lett. 49, 57 (1982).

The Si (111) reconstruction

Si (111) annealed at 1000°C, slow cooling-down.

First atomic resolution

STM gave the exact nature of the surface left unknown by LEED exp.

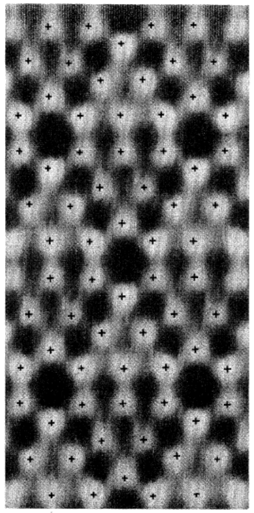

FIG. 2. Top view of the relief shown in Fig. 1 (the hill at the right is not included) clearly exhibiting the sixfold rotational symmetry of the maxima around the rhombohedron corners. Brightness is a measure of the altitude, but is not to scale. The crosses indicate adatom positions of the modified adatom model (see Fig. 3) or "milk-stool" positions (Ref. 5).

Hard-paper work from trace-recorder data.

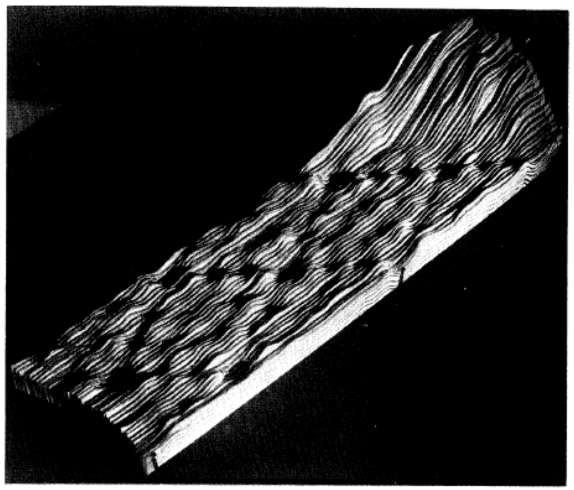

FIG. 1. Relief of two complete 7×7 unit cells, with nine minima and twelve maxima each, taken at 300 °C. Heights are enhanced by 55%; the hill at the right grows to a maximal height of 15 Å. The $[\bar{2}11]$ direction points from right to left, along the long diagonal.

"7x7 reconstruction on Si (111) resolved in real space", G. Binnig, H. Röhrer, Ch. Gerber and E. Weibel, Phys. Rev. Lett. 50, 120 (1983).

Nobel prize 1987.

Si (111) 7x7 : the model

In the bulk, diamond-like structure.

7x7 reconstruction minimizes nb of pending bonds : 49->19

Miller index refer to the number (= 7) of atomic cells involved.

In STM, the adatoms only are visible, a well as the corner vacancies.

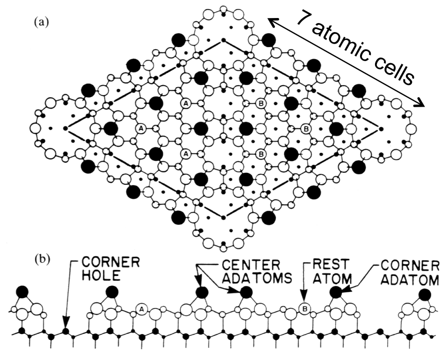

Fig. 4.2. DAS model of the Si(111) (7×7) surface. (*a*) Top view. Atoms o (111) layers at decreasing heights are indicated by circles of decreasing size Heavily outlined circles represent 12 adatoms. Larger open circles represei atoms in the stacking fault layer. Smaller open circles represent atoms in th dimer layer. Solid circles and dots represent atoms in the unreconstructed laye beneath the reconstructed surface. (*b*) Side view. Larger open and solid circle indicate atoms on the $(\bar{1}01)$ plane parallel to the long diagonal across the corne vacancies of the (7×7) unit cell. Smaller open and solid circles indicate atom on the next $(\bar{1}01)$ plane (Takayanagi *et al.*, 1985b).

Si (111) 7x7

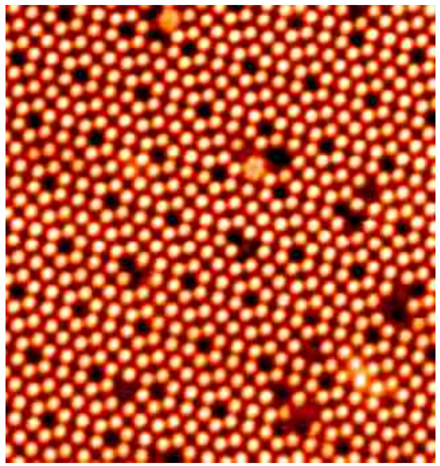

Single vacancies, adsorbates, screw dislocations are visible: true atomic resolution. (Omicron website)

Chapter 3
Imaging with a STM

3.1: Imaging at different bias

The chemical contrast: GaAs (110)

Two superposed images:

occupied states: $V_{sample} < 0$, red level: As.

+

empty states: $V_{sample} > 0$, green level: Ga

Images are taken simultaneously to avoid hysteresis effects between two succesive images.

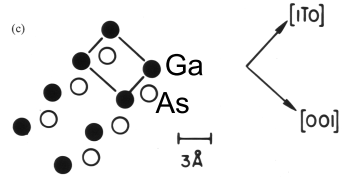

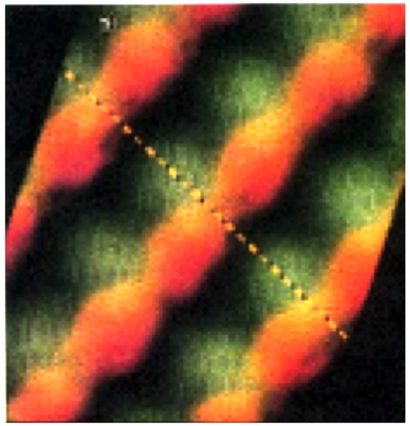

J. Stroscio et al, Phys. Rev. Lett. 58, 1192 (1987).

Occupied / empty states: a naive picture

As potential more attractive than Ga.
Close to Fermi level, occupied states are on As, empty ones on Ga.

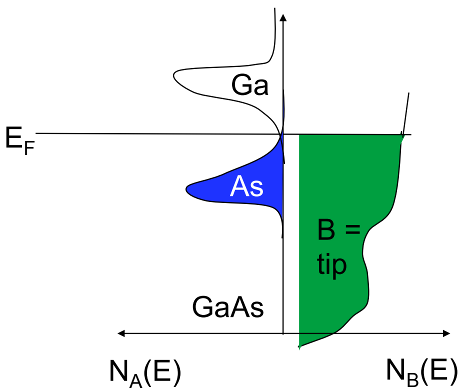

eV > 0: As atoms are imaged.
eV < 0: Ga atoms are imaged.

Depending on bias, occupied or empty states participate to tunneling: complementary information can be accessed.

Occupied / empty states: a naive picture

As potential more attractive than Ga.
Close to Fermi level, occupied states are on As, empty ones on Ga.

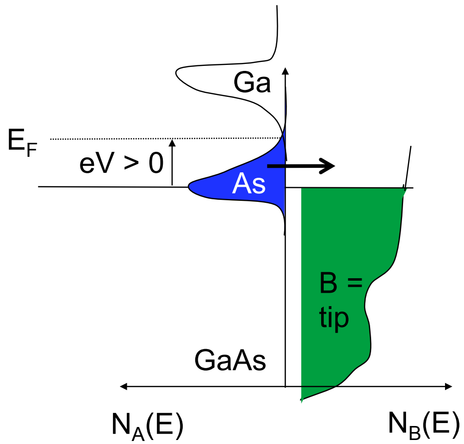

eV > 0: As atoms are imaged.
eV < 0: Ga atoms are imaged.

Depending on bias, occupied or empty states participate to tunneling: complementary information can be accessed.

Occupied / empty states: a naive picture

As potential more attractive than Ga.
Close to Fermi level, occupied states are on As, empty ones on Ga.

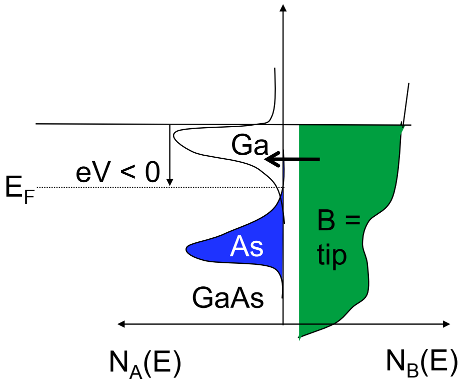

eV > 0: As atoms are imaged.
eV < 0: Ga atoms are imaged.

Depending on bias, occupied or empty states participate to tunneling:
complementary information can be accessed.

Real-time dynamics of Pb atoms on Si

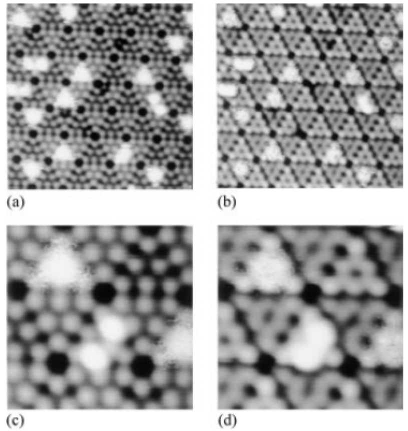

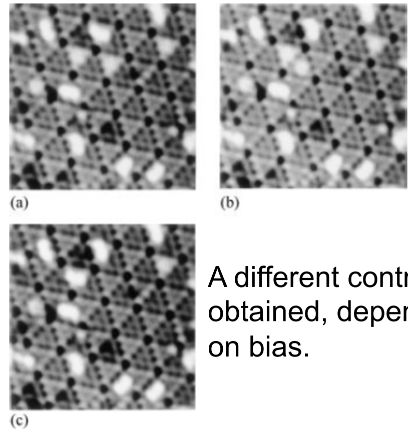

A different contrast is obtained, depending on bias.

FIG. 1. Filled and empty state STM images of 0.01 ML Pb on Si(111)-(7 × 7) measured at room temperature. The scanning areas are 16.25 × 16.25 nm² [(a) and (b)] and 6.0 × 6.0 nm² [(c) and (d)]. Sample voltages are +2 V [(a) and (c)] and −2 V [(b) and (d)]. Tunnel current is 0.2 nA for all images.

FIG. 2. Successive frames extracted from an STM movie measured at 58 °C, showing the jump of a single Pb atom (b) and the formation of a pair (c). The time between frames is 25 sec. The scanning area is 14.75 × 14.75 nm². Sample voltage: −2 V. Tunnel current: 0.2 nA.

J.-M. Rofriguez-Campos et al, Phys. Rev. Lett. 76, 799 (1996), Institut Néel, Grenoble.

Three / six-fold symmetry in graphite

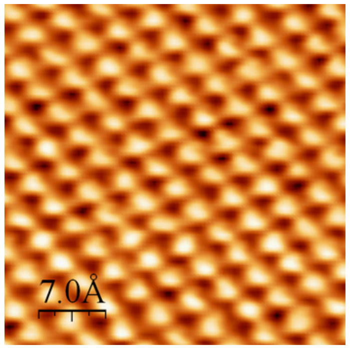

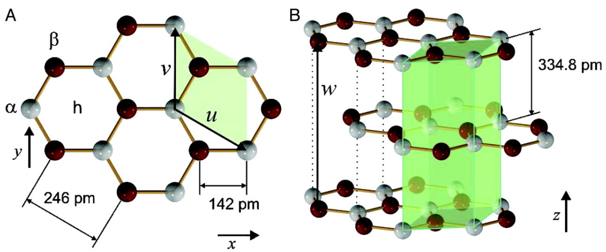

Clean surface thanks to the layered structure and scotch technique.

STM images display a triangular lattice, not a hexagonal one:
coupling with the second layer make every other two atom “different”.

STM images not the atoms but the electronic clouds.

Moiré in graphene

UHV annealing of SiC,

epitaxy on Re:

formation of a graphene sheet on a crystalline substrate.

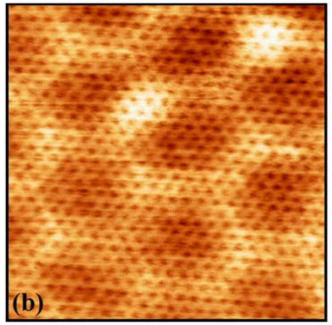

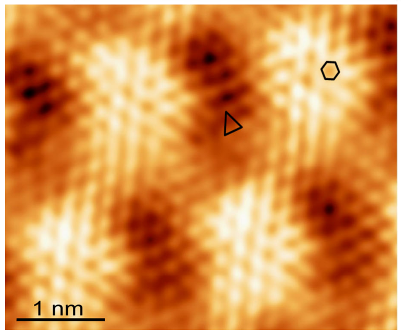

Atomic lattice visible, 6-fold periodicity.

Images shows electronic interference effects with the buffer layer: moiré.

P. Mallet, J.Y. Veuillen et al, Phys. Rev. B 76, 041403(R) (2007), Institut Néel. C. Tonnoir et al, Phys. Rev. Lett. 111, 246805 (2013), INAC.

Chapter 4
Scanning Tunneling Spectroscopy

4.1 Superconductors

Elements of superconductivity (1)

A superconductor (below T_c, I_c and B_c):
- zero resistance,
- perfect diamagnetism (B = 0),
- modified density of states at the FL,

BCS theory : the DOS writes :

$$N_S(E) = 0 \quad \text{if} \left|E - E_F\right| < \Delta$$

$$N_S(E) = N_N \frac{\left|E\right|}{\sqrt{\left(E - E_F\right)^2 - \Delta^2}} \quad \text{if} \left|E - E_F\right| > \Delta$$

The energy gap is :
$\Delta(T\text{->}0) = 1.76 k_B T_c$

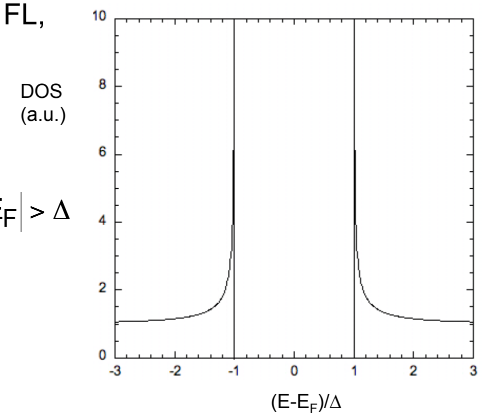

$NbSe_2$

Lamellar compound,

Easy to cleave (scotch tape): gives a clean, inert surface.

Superconducting below 7.2 K.

Spectra follows BCS shape.

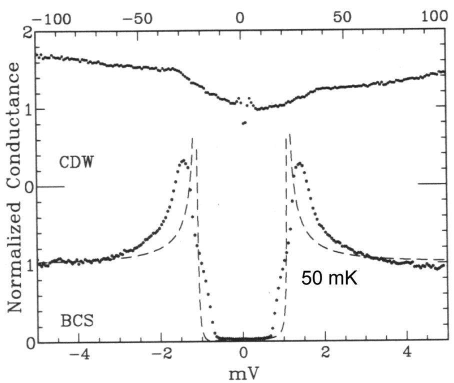

H.F. Hess et al., Physica B 169, 422 (1991).

Elements of superconductivity (2)

Type II : magnetic field penetration length λ_L > coherence length ξ_s.

In $NbSe_2$, : ξ_s = 77 Å, λ_L = 2000 Å.

A superconductor under magnetic field: magnetic field penetrates as vortices made of a normal core,each vortex carries a flux quantum ϕ_0.

When field increases, the number of vortices increases accordingly.

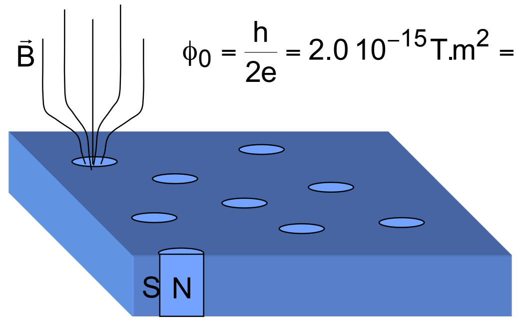

$$\phi_0 = \frac{h}{2e} = 2.0\,10^{-15}\,T.m^2 = 2.0\,mT.\mu m^2$$

Inside a vortex

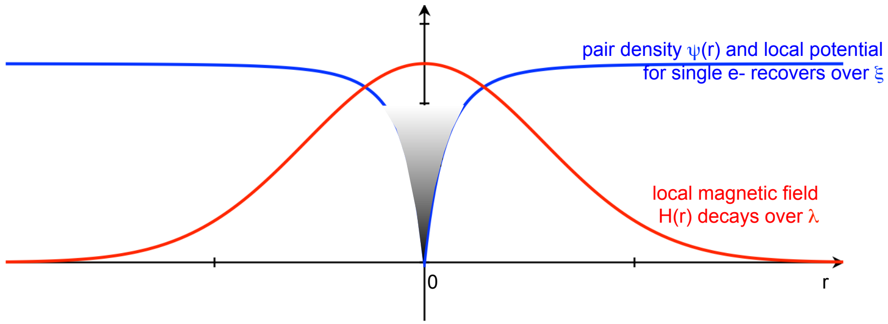

Local magnetic field depletes Cooper pair density and pairing potential:
localized (single-)electron states,
local density of states modified.

Localized states in a vortex

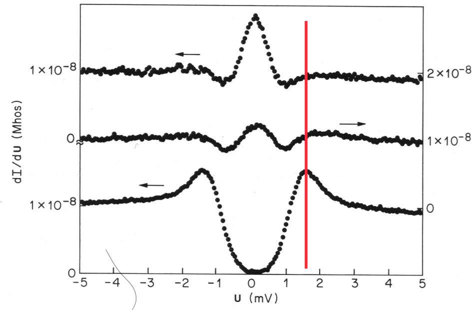

Fig. 4.121. Plot of dI/dU versus U for $NbSe_2$ at 1.85 K and 0.02 T field, taken at three different positions: on a vortex, about 75 Å from a vortex, and 2000 Å from a vortex (Hess *et al.*, 1989).

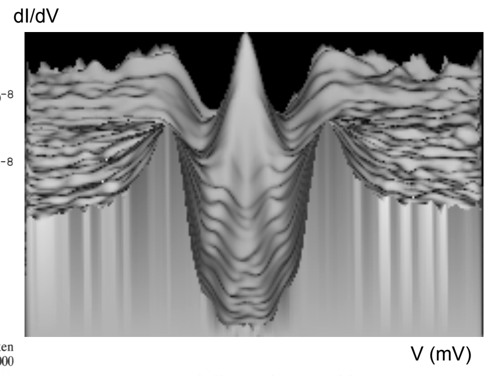

Series of LDOS spectroocopy along a line across a vortex:
quasiparticules states confined within a vortex core = LDOS peak.

H.F. Hess et al., Phys. Rev. Lett. 64, 2711 (1990).

The differential conductance imaging

During scan: ac modulation V_{ac} added to dc bias V_{dc}.

$$V = V_{dc} + V_{ac0} \cos \omega t$$

Regulation slower than ac modulation ⇨ ac current modulation.

$$I = I(V_{dc}) + \left.\frac{dI}{dV}\right|_{V=V_{dc}} .V_{ac0} \cos \omega t$$

dI is measured and displayed (with grey levels).
Bias V_{dc} well chosen so that dI/dV image reflects the LDOS structure.

Also called STS map.

The vortex lattice

Abrikosov (Nobel 2003) vortex lattice.

Triangular geometry: interaction between vortices is minimized.

Vortex density determined by the magnetic field.

H.F. Hess et al., Phys. Rev. Lett. 62, 214 (1989).

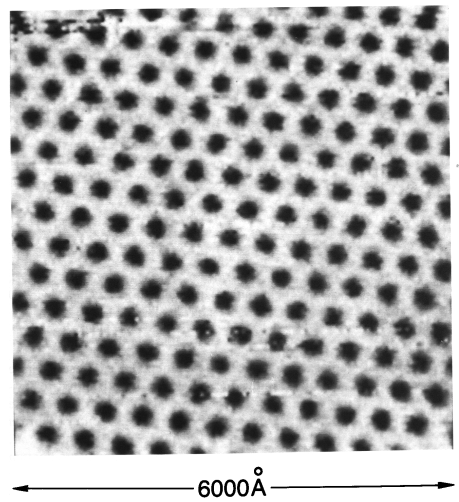

Fig. 4.120. Abrikosov flux lattice produced by 1 T magnetic field in $NbSe_2$ at 1.8 K. The gray scale corresponds to dI/dU (Hess *et al.*, 1989).

Chapter 4
Scanning Tunneling Spectroscopy

4.2 Single-wall carbon nanotubes

Structure

Discovered in 1991: S. Iijima et al., Nature 354, 56 (1991).

Wrapped graphene sheet with a rolling vector:

$$\vec{R} = n\vec{a}_1 + m\vec{a}_2$$

(n,m) defines the tube geometry.

n = m : armchair
m = 0 : zig-zag
n ≠ m chiral

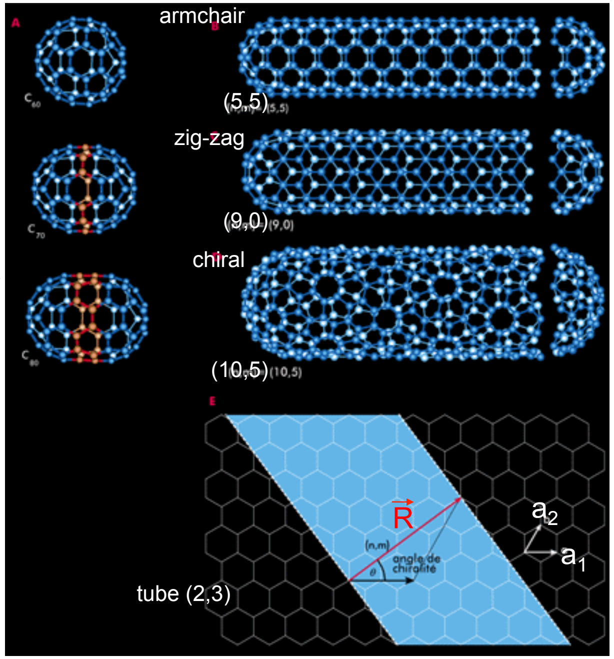

Electronic states in graphene (1)

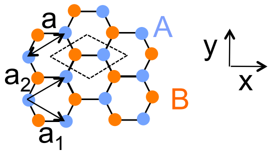

Two atoms per unit cell (diamond), A and B.
a = 0.246 nm

sp^2: s, p_x and p_y hybridize to form σ states, which are in-plane, occupied by 3 electrons. p_z states allow conduction: to be considered in the following, occupied by one electron per atom.

Tight binding approx.: electrons tighly bound to their atom, electronic states are a combination of p_z atomic orbital.

Electronic states in graphene (3)

$$E(k) = \pm t\left[3 + 2\cos(k_y a) + 4\cos\left(\sqrt{3}k_x a/2\right)\cos(k_y a/2)\right]^{1/2}$$

t = 2.5 eV (nearest neighbour transfer integral).

One e- in the binding orbital E < 0.

Fermi level made of 6 points K: intrinsic graphene is a semi-metal or gapless semiconductor.
Close to FL, linear relation dispersion: Dirac fermions.

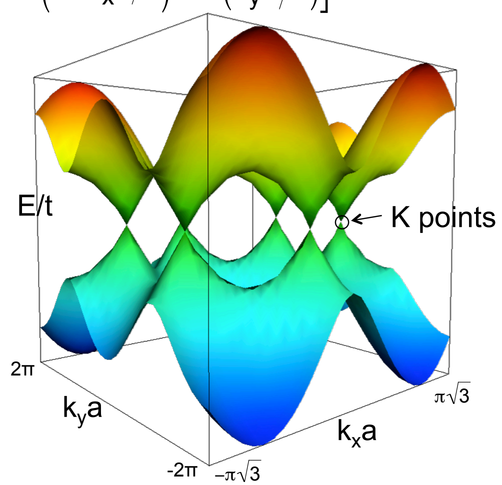

P. R. Wallace, Phys. Rev. 71, 622 (1947).

Armchair tubes are metallic

Armchair, periodic boundary condition around the perimeter:

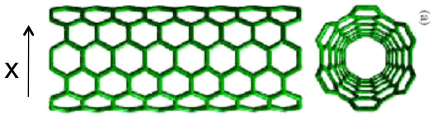

$k_x.m\sqrt{3}a = 2\pi p$ p integer

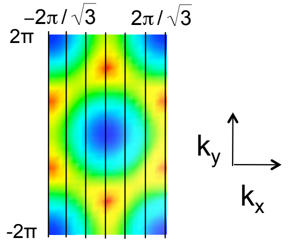

m = 3

$$k_x a = \frac{2\pi p}{m\sqrt{3}}$$

K points in red in this figure.
Selected k_x cross K points: metallic.

Zig-zag can be metallic or semiconducting

Zig-zag, periodic boundary condition around the perimeter:

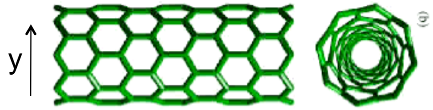

$k_y.na = 2\pi p$ p integer

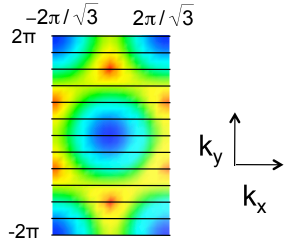

n = 6: metallic CNT

$$k_y a = \frac{2\pi p}{n}$$

K points in red in this figure.
Selected k_y cross K points or not, depending on m.

Zig-zag can be metallic or semiconducting

Zig-zag, periodic boundary condition around the perimeter:

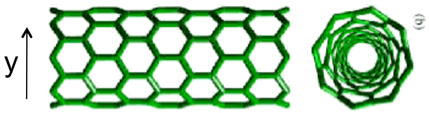

$k_y.na = 2\pi p$ p integer

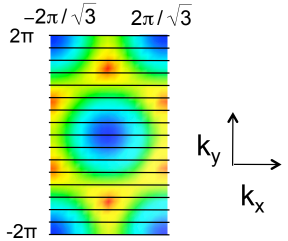

n = 8: semiconducting CNT

$$k_y a = \frac{2\pi p}{n}$$

K points in red in this figure.
Selected k_y cross K points or not, depending on m.

Chiral nanotubes …

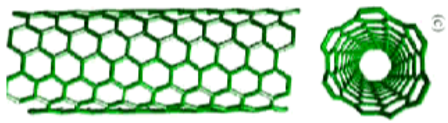

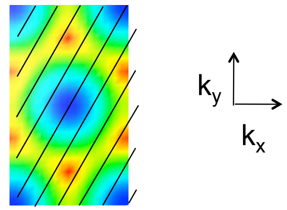

Boundary condition:
$k_x.m\sqrt{3}a + k_y.(n-m)a = 2\pi p$

Selected k_x,k_y lines can cross K points, depending on (m,n), in which case the CNT is metallic.

Theoretical prediction:

n - m = 3k : metallic,
n - m ≠ 3k : semiconductor.

CNT imaging

CNTs on a Au surface.

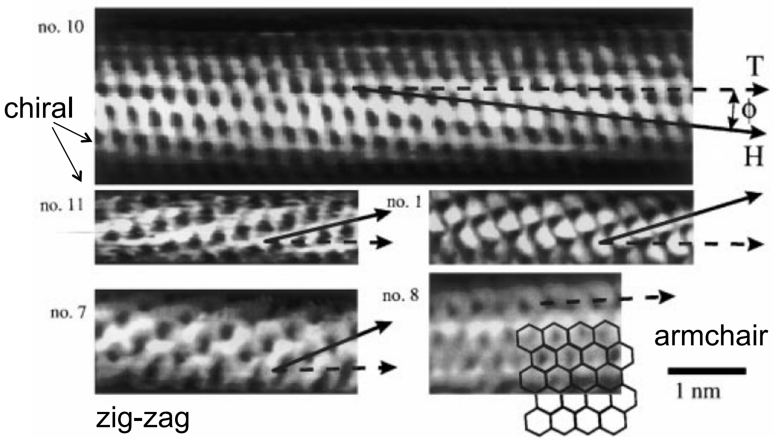

J.W.G. Wildoer, C. Dekker et al, Nature 391, 59 (1998).

CNT spectroscopy

Metallic and semiconducting tubes identified.

Armchair tubes found metallic. Statistics agrees with 1/3 of chiral ones being metallic.

Energy gap in SC tubes:

$$E_{gap} = 2\gamma a / \sqrt{3} d$$

d: tube diameter.

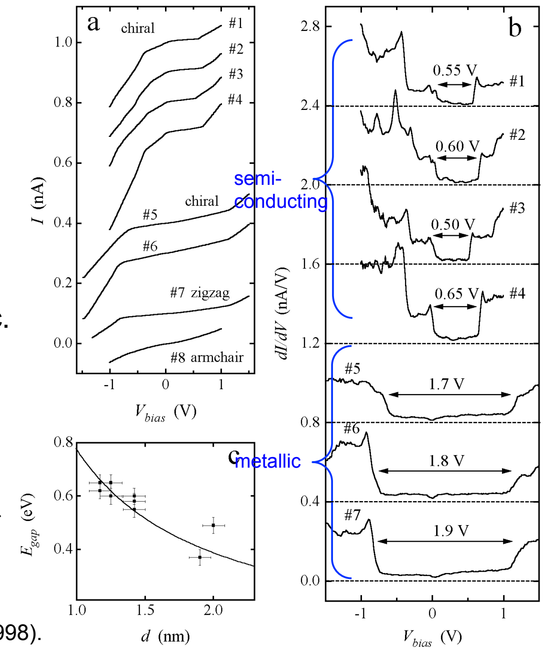

J.W.G. Wildoer et al, Nature 391, 59 (1998).

Imaging electron wave functions in a CNT (1)

Armchair (metallic) tube cut with a 5V voltage pulse:

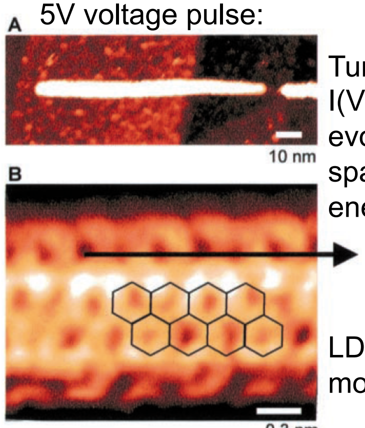

Tunnel contact I(V) and dI/dV evolves spatially at low energy.

LDOS spatial modulation.

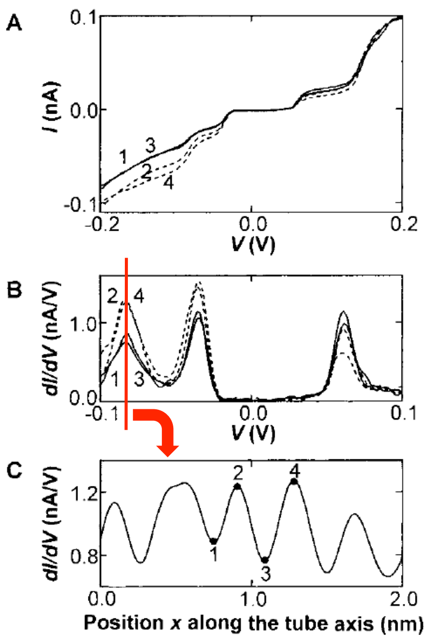

L. C. Venema et al, Science 283, 52 (1999).

Imaging electron wave functions in a CNT (2)

Period different from atomic cell size, close to Fermi wavelength: electronic standing waves.

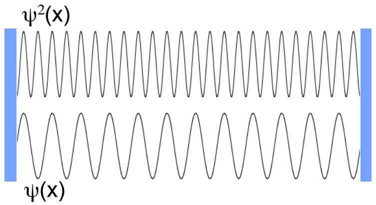

$$\psi(x) = A \sin(2\pi x/\lambda)$$

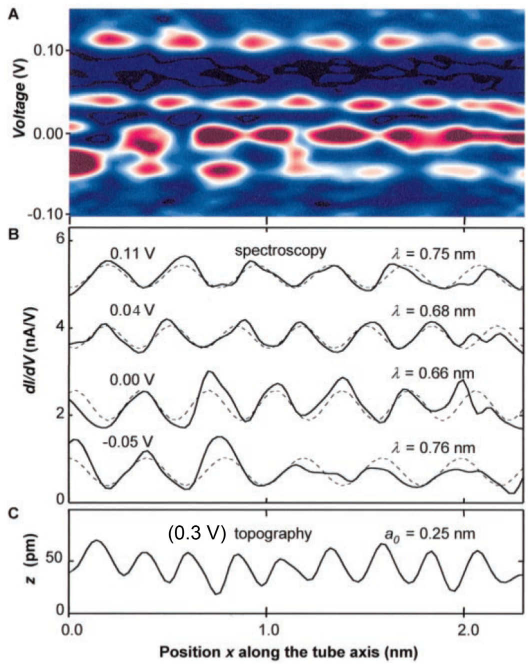

Imaging electron wave functions in a CNT (2)

Differential conductance proportional to electron density:

Fit: $\frac{dI}{dV} = G_1 \sin^2(2\pi x/\lambda) + G_0$

Textbook model of a particle in a 1D box, here about 100 e-.